



Synthesis and Optical Properties of Lanthanum Doped Nanocrystalline Tin Dioxide Thick Films

L.P.Chikhale^{*1}, F.I.Shaikh², A.V.Rajgure³, S.S.Suryavanshi⁴

^{*1}Department of Physics, Venkatesh Mahajan Senior College, Osmanabad, Maharashtra, India

²Department of Physics, Government Institute of Forensic Science, Aurangabad, Maharashtra, India

³G.S.Tompe Arts, Commerce & Science College, Chadur Bazar, Dist-Amravati 444704, Maharashtra, India

⁴Department of Physics, Solapur University, Solapur, Maharashtra, India

ABSTRACT

To study the effect of pure and La doped tin dioxide thick films on their optical properties and the oxide powders were prepared by the chemical co-precipitation method. The thick films of La doped SnO₂ were prepared by the screen-printing technique and further sintered at 750° C. The samples were characterized by X-ray diffraction (XRD), thermo gravimetric-differential thermal analyzer (TG-DTA) and Fourier transformation infrared spectroscopy (FTIR) and UV-VIS techniques. XRD studies reveal formation of fine nanocrystalline material. The particle size of sintered powder of pure and La (2 and 4 mol %) doped SnO₂ powders were 15, 10 and 9 nm respectively. These results were further confirmed by FTIR studies. Crystallite size was observed to vary from 16 to 9 nm as the La content increased from 0 to 4 mol%, suggesting the prevention of crystal growth with La doping. It was evident from the absorption spectra that the absorbance increases with the dopant concentration. Optical band gap was estimated by using Tauc relation which decreases with the increase in La content confirming the size reduction as a result of La doping. Raman spectroscopic measurements showed that the broadening of intense peak observed at 647 cm⁻¹ with La doping, indicating that the La ions are substituted at the Sn sites in SnO₂ lattice.

Keywords: Tin oxide; Thick film; Screen printing; Lanthanum

I. INTRODUCTION

In catalyst, it is desirable to produce materials with nanometric-scale structures to obtain improvement in some specific properties [1]. To prepare active nanocrystalline powders, several chemical techniques have been investigated and reported in the literature. Among the various methods of preparation of nanostructured SnO₂, polymeric precursor method [2], sol-gel method [3], hydrothermal method [4], electrospinning technique [5], co-precipitation [6], chemical vapor deposition (CVD)[7], sol-gel method[8], combustion method[9], spray pyrolysis technique [10] etc. are popular. Many workers proposed the use of nanocrystallite of SnO₂ in thin film form and reported that SnO₂ thin films can have maximum gas sensitivity only if the crystallite size of the film is comparable with its space-charge thickness which is below 10 nm [14].

The purpose of the present work is to investigate the effect of La doping SnO₂ on its structural, morphological and optical properties. We have chosen La as dopant material as it is catalytically active material and has been investigated by several researchers [15].

II. EXPERIMENTAL PROCEDURE

The details of the preparation of undoped and doped SnO₂ powder as well as thick film technique are described elsewhere [16].

2.1. Characterization:

The thermal analysis of the prepared powder was obtained by thermo gravimetric differential thermal analysis (TG-DTA) performed on SDT Q600 V20.9 Build20 instruments in ambient air with increasing the temperature at a rate of 10° C /min. The structural properties of pure and La doped SnO₂ thick films are studied by computer controlled X-ray diffractometer (BRUKER AXS D8-Advanced) using Cu-K α ($\lambda=1.54056$ Å) radiation. The scanning angle 2θ was in the range of 20° to 90°. The average crystallite size (D) of sintered pure and La doped SnO₂ was estimated using the Scherrer equations as follows:

$$D = \frac{0.9\lambda}{\beta \cos\theta} \dots\dots\dots (2)$$

Where, λ , β and θ are the X-ray wavelength, the full width at half maximum (FWHM) of the diffraction peak, and the Bragg's diffraction angle respectively.

The UV-absorption spectra of pure SnO₂ and La doped SnO₂ were performed using JASCO (Model V-670) UV-VIS-NIR spectrophotometer. The spectra were taken in the wavelength range of 200-1000 nm for studying the optical band-gap of the samples. FTIR spectroscopic measurements of sample powder sintered at 750°C in air has been studied in the wave number range of 400-4000 cm⁻¹, using JASCO Model FTIR -6100 type spectrophotometer for studying the chemical groups on the surface of samples.

III. RESULTS AND DISCUSSION

3.1. TGA and DTA analysis:

Fig. 1 shows the TG-DTA curves of as prepared powder for L2. Significant weight loss was observed from room temperature to 300°C. The weight change up to temperature of 300°C was due to release of adsorbed water, crystal water and other gases which was also observed as weak endothermic peak in DTA curve. Above 600°C there is no weight loss indicating phase formation of L2. From the TGA-DTA studies we have opted 750°C as a optimum sintering temperature for pure and La doped SnO₂ samples.

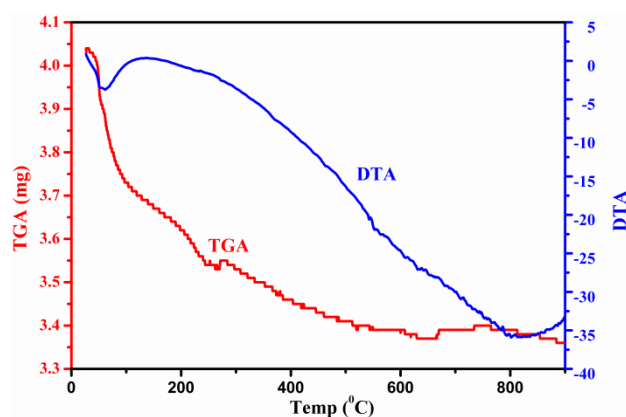


Fig.1 TGA-DTA profile of the precipitate precursor of pristine SnO₂.

3.2. XRD analysis:

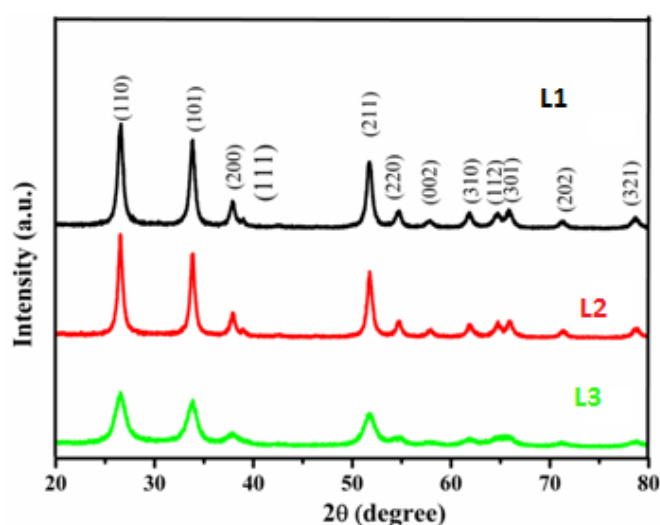


Fig. 2 XRD patterns of undoped (L1) , 2 mol % La-doped (L2) , and 4 mol % La-doped SnO₂ (L3).

Fig. 2 show the XRD patterns of SnO₂ thick films with different La concentrations. All patterns exhibit peaks corresponding to the rutile structure of polycrystalline SnO₂ with the maximum intensity peak corresponding to (110) planes and are indexed on the basis of joint committee on powder diffraction standards (JCPDS) data [17]. However, the relative intensity of the peaks decreases with an increase in the La content. It is also observed that the full width at half maxima (FWHM) of the diffraction peaks increases with increasing La content which is in good agreement with the earlier studies [18]. The increase in FWHM along with a decrease in peak intensity suggests that La incorporation into the SnO₂ lattice results in a decrease in crystallite size of the films. The decrease in the crystallite size is further supported by the decrease in the sharpness of the peaks with the incorporation of La. Pure SnO₂ has an average crystallite size of 15nm, while 2 mol % La doped SnO₂ shows reduced crystallite size of 10 nm and 8 nm in case of 4mol % La-doped SnO₂.

3.3. Optical analysis:

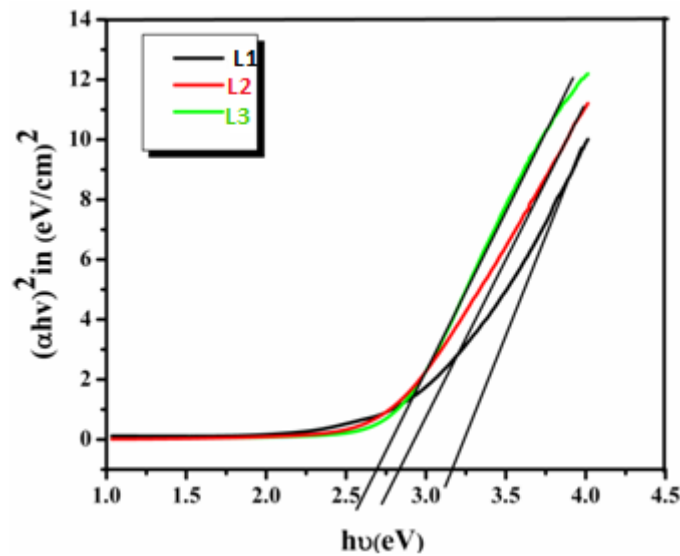


Fig. 3 UV spectra of undoped (L1) , 2 mol % La-doped (L2) , and 4 mol % La-doped SnO₂ (L3)

UV absorption spectra were carried out on the JASCO Model V-670 Spectrophotometer in the wavelength range 200-1000nm. Fig.3 shows the optical absorbance spectra for of pure and La doped SnO₂ powder samples sintered at 750°C in the wavelength range 200–1000 nm. The nature of the transition is determined by using the relation:

$$\alpha = \text{const} \times \frac{(hv - E_g)^{1/2}}{hv} \dots\dots\dots (2)$$

Where, E_g is the optical band gap energy which was calculated from $(\alpha hv)^2$ versus energy ($h\nu$) plot, A is a constant, α is the absorption coefficient, $h\nu$ is the photon energy taken from the UV-spectra. The plot of $(\alpha hv)^2$ as a function of the energy ($h\nu$) of the incident radiation has been shown in Fig. 3. It is found that the nature of the plot is nonlinear indicating absence of indirect transition. The band edge can be evaluated from the intercept of the extrapolated linear part of the curve with the energy axis. The corresponding value of the optical band gap (E_g) for pristine SnO₂ is found to be 3.17 eV. La doping also has influence on optical band gap of the La-doped SnO₂ films. Data from this study showed the direct optical band gap of La-doped SnO₂ thick films for La-doping levels in the range 0 to 4 mol% were found to be 3.17 to 2.69 eV respectively (Fig. 3). It should be noted that reduction in optical band gap was observed after La doping which is consistent with the direct optical band gap of various La doped SnO₂ thick films reported by [19]. The reason for optical band gap reduction might be due to the appearance of the La-Sn metallic compounds, as seen in XRD analysis results.

3.4. FTIR analysis

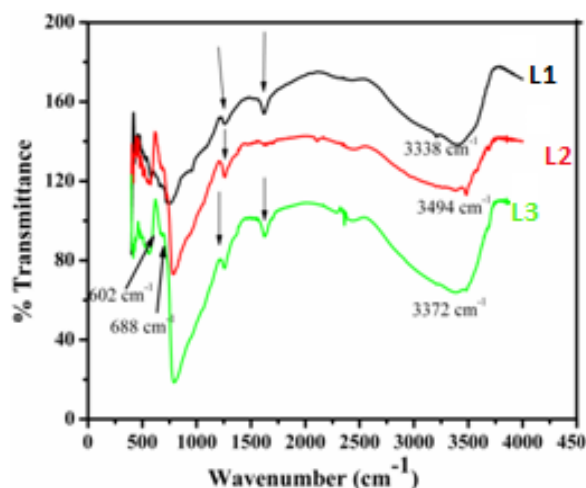


Fig. 4 Shows the FTIR spectrum for studying the chemical composition on the surface of the samples L1, L2, and L3 sintered at 750°C in air after mixing in KBr powder. All FTIR spectra contain absorption bands in the range of 2500–3500 cm^{-1} associated with water and absorption of Sn-OH groups. The peak which appeared at 602 cm^{-1} relates to the terminal oxygen vibration of Sn-OH, while the peak appearing at 688 cm^{-1} is due to the O-Sn-O bridge functional group of SnO₂ (L1). The broad band centered on 3250 cm^{-1} region is due to the stretching vibration of O-H (Sn-OH) bond [20]. Addition of dopants changed the positions of two characteristic vibration peaks of the Sn-O bond in SnO₂ [21]. The sample doped with La (L2) changed the positions of these two peaks to 776 cm^{-1} and 1200 cm^{-1} , respectively. The positions of these two peaks changed to 741 cm^{-1} and 957 cm^{-1} , respectively in the La doped SnO₂ (L3). The additional absorption peaks were observed with La addition, indicating its homogeneous dispersion in the support material.

IV. CONCLUSIONS

The films of co precipitation synthesized undoped and La doped SnO₂ were successfully deposited using screen printing technique. The XRD, UV-Vis, FTIR spectroscopic analysis confirmed that the La doping in SnO₂ can significantly affects particle size and band gap of La doped SnO₂. These results indicate that the La doped SnO₂ material can be used as a potential candidate for fabricating the optoelectronic devices.

V. REFERENCES

- [1]. D. Wang, J. Jin, D. Xia, Q. Ye, J. Long, The effect of oxygen vacancies concentration to the gas-sensing properties of tin dioxide-doped Sm. *Sensors and Actuators B* 66 (2000) 260–262
- [2]. A.P. Maciel, P.N. Lisboa-Filho, E.R. Leite, C.O. Paiva-Santos, W.H. Schreiner, Y. Maniette, E. Longo, Microstructural and morphological analysis of pure and Ce-doped tin dioxide nanoparticles, *Journal of the European Ceramic Society* 23 (2003) 707–713.

- [3]. G. T. Ang, G. Hoon Toh, M. Z. Abu Bakar, A. Z. Abdullah, M. R. Othman. High sensitivity and fast response SnO₂ and La-SnO₂ catalytic pellet sensors in detecting volatile organic compounds, *Process Safety and Environmental Protection* 89 (2011) 186–192.
- [4]. P. Sun, Y. Cao, J. Liu, Y. Sun, J. Ma, G. Lu. Dispersive SnO₂ nanosheets: Hydrothermal synthesis and gas-sensing properties, *Sensors and Actuators B* 156 (2011) 779–783.
- [5]. H. Zhang, Z. Li, L. Liu, X. Xu, Z. Wang, W. Wang, W. Zheng, B. Dong. Enhancement of hydrogen monitoring properties based on Pd-SnO₂ composite nanofibers, *Sensors and Actuators B* 147 (2010) 111–115.
- [6]. J. Zhang, S. Wang, Y. Wang, M. Xu, H. Xia, S. Zhang, W. Huang, X. Guo, S. Wu. Facile synthesis of highly ethanol sensitive SnO₂ nanoparticles, *Sensors and Actuators B* 139 (2009) 369–374.
- [7]. H. T. Feng, R. F. Zhuo, J. T. Chen, D. Yana, J. J. Feng, H. J. Li, S. Cheng, P. X. Yan. Axial periodical nanostructures of Sb-doped SnO₂ grown by chemical vapor deposition, *Physica E* 41 (2009) 1640–1644.
- [8]. M. Hubner, S. Hafner, N. Barsan, U. Weimar. The influence of Pt doping on the sensing and conduction mechanism of SnO₂ based thick film, *Sensors Procedia Engineering* 25 (2011) 104 – 107.
- [9]. A. Ayeshamariam, C. Sanjeeviraja, M. Jayachandra. Synthesis, characterization and gas sensing properties of SnO₂ nanoparticles, *International Journal of Chemical and Analytical Science* 2(6) (2011) 54-61.
- [10]. V. Brinzari, G. Korotcenkov, V. Golovanov, J. Schwank, V. Lantto, S. Saukko, Morphological rank of nano-scale tin dioxide films deposited by spray pyrolysis from SnCl₄.5H₂O water solution, *Thin Solid Films* 408 (2002) 51–58.
- [11]. Z. Wang, L. Liu. Synthesis and ethanol sensing properties of Fe doped SnO₂ nanofibers, *Materials Letters* 63 (2009) 917–919.
- [12]. K. Galatsis, L. Cukrov, W. Wlodarski, P. McCormick, E. Comini, G. Sberveglieri. p- and n-type Fe-doped SnO₂ gas sensors fabricated by the mechanochemical processing technique, *Sensors and Actuators B* 93 (2003) 562–565.
- [13]. S. Chakraborty, A. Sen, H.S. Maiti, Selective detection of methane and butane by temperature modulation in iron doped tin oxide sensors, *Sensors and Actuators B* 115 (2006) 610–613.
- [14]. S. Bose, S. Chakrabortya, B.K. Ghoshb, D. Dasc, A. Sena, H.S. Maitia, Methane sensitivity of Fe-doped SnO₂ thick films, *Sensors and Actuators B* 105 (2005) 346–350.
- [15]. L.A. Patil, D.R. Patil, Heterocontact type CuO-modified SnO₂ sensor for the detection of a ppm level H₂S gas at room temperature, *Sensors and Actuators B* 120 (2006) 316–323.
- [16]. L.K. Bagal, J.Y. Patil, I.S. Mulla, S.S. Suryavanshi, Influence of Pd-loading on gas sensing characteristics of SnO₂ thick films, *Ceramics International* 38 (2012) 4835–4844.
- [17]. JCPDS Data Card No.14-4145.
- [18]. S. Rani, S. C. Roy, M.C. Bhatnagar. Effect of Fe doping on the gas sensing properties of nano-crystalline SnO₂ thin films, *Sensors and Actuators B* 122 (2007) 204–210.
- [19]. N. Timonah, C. Yang, L. Sun, Structural, optical and electrical properties of Fe doped SnO₂ fabricated by sol-gel dip coating technique, *Materials Science in Semiconductor Processing* 13 (2010) 125–131.

- [20]. M.V. Vaishampayan, R.G. Deshmukh, P.Walke, I.S. Mulla, Fe-doped SnO₂ nonmaterial: A low temperature hydrogen sulfide gas sensor, *Materials Chemistry and Physics* 109 (2008) 230–23416.
- [21]. M. M. Bagheri-Mohagheghi, N. Shahtahmasebi, M.R. Alinejad, A. Youssefi, M. Shokooh-Saremi, Fe-doped SnO₂ transparent semi-conducting thin films deposited by spray pyrolysis technique: Thermoelectric and p-type conductivity properties, *Solid State Sciences* 11 (2009) 233-239.
- [22]. R.Adnan, N.A. Razana, I. A.Rahman, M. A.Farrukh, Synthesis and characterization of high surface area tin oxide nanoparticles via the sol-gel method as a catalyst for the hydrogenation of styrene, *Journal of the Chinese Chemical Society*, (2010) 222-229.
- [23]. L. S. Chuah, M. Y. Yaacob, M. S. Fan, S. S. Tneh, Z. Hassa, Synthesis, characterization and optical properties of Ni-doped nanocrystalline SnO₂, *Optoelectronics and Advanced Materials*, Vol. 4, No. 10, October 2010, p. 1542 – 1545.